

Anomalous Hall effect revisited

A. Crépieux* and P. Bruno

Max-Planck-Institut für Mikrostrukturphysik, Weinberg 2, 06120 Halle, Germany

(December 2, 2024)

A model to calculate the anomalous Hall effect is developed. Based on the Dirac equation and on the Kubo formalism, this model allows to calculate simultaneously the skew-scattering and side-jump contributions to the anomalous Hall resistivity. The continuity and the consistency with the weak-relativistic limit described by the Pauli Hamiltonian is shown. For both approaches, Dirac and Pauli, the Feynmann diagrams, which lead to the skew-scattering and the side-jump contributions, are underlined. In order to illustrate this method, we apply it to a particular case: a ferromagnetic bulk alloy in the limit of weak disorder and free-electrons approximation. Explicit expressions of the anomalous Hall conductivity for both skew-scattering and side-jump mechanisms are obtained.

I. INTRODUCTION

In magnetic metals, in addition to the normal part proportional to the magnetic field, the Hall resistivity contains a supplementary part proportional to the magnetization which is called anomalous Hall resistivity:

$$\rho_H = R_0 H + R_S M, \quad (1)$$

where R_0 and R_S are respectively the normal and anomalous Hall coefficients, H is the magnetic field and M the magnetization. While the normal Hall effect results from the Lorentz force, the anomalous Hall effect is due to the spin-orbit coupling in presence of spin polarization. Experimentally, the normal and anomalous parts can be extracted by measuring the Hall resistivity according to the magnetic field. At high magnetic field, when the magnetic saturation is reached, we get a linear variation of the Hall resistivity with a slope related to R_0 and an extrapolated value at zero magnetic field related to R_S . Experimentally, the normal and anomalous Hall coefficients have been determined for a large number of bulk alloys. These studies¹⁻⁵ reveal that the sign of R_S can changes according to the alloy composition and that $|R_S|$ is generally larger than $|R_0|$.

For different reasons, renewed consideration to the anomalous Hall effect is observed quite recently. It is not only due to the increasing interest in spin-dependent transport phenomena but also because of some particular and interesting behaviours of the anomalous Hall resistivity obtained experimentally in granular alloys⁶, in magnetic films⁷ and multilayers⁸. In addition, the anomalous Hall effect is increasingly used as a measurement tool to detect for example magnetization⁹, dynamics of magnetic domains¹⁰ or perpendicular anisotropy¹¹.

In the sixties, a number of theoretical works¹²⁻¹⁵ attempted to elucidate the physical mechanisms responsible for the anomalous Hall effect and to calculate an explicit expression of the anomalous Hall resistivity. A series of controversies¹⁶⁻¹⁸ have been generated by these pioneer works which were, for some of them, resolved by detailed calculations^{19,20} and comparisons²¹. It is now generally accepted²² that two mechanisms are responsible for

the anomalous Hall effect: the skew-scattering proposed by Smit¹³ and the side-jump proposed by Berger¹⁵. An illustrative picture of these mechanisms is given on Fig. 1. Consider an incident plane-wave characterized by a wave-vector \mathbf{k} which is scattered by a central potential due to impurity. In presence of spin-orbit coupling, the amplitude of the wave-packet becomes anisotropic in the sense that it depends of the relative directions between the incident plane-wave and the spin. After a succession of scattering, the average trajectory of the electron is deflected by a spin-dependent angle which is typically of order 10^{-2} rad. This first mechanism, depicted by the schema (a) on Fig. 1, corresponds to the skew-scattering. The second mechanism corresponds to a lateral displacement $\delta \approx 10^{-11}$ m of the center of the wave-packet during the scattering, which is also spin-dependent. This mechanism, depicted by the schema (b) on Fig. 1, corresponds to the side-jump. In both cases, due to the spin-orbit coupling, the effect is asymmetrical in respect to the spin state. The spin up current and spin down current are then different. In magnetic material, this lead to a non-zero spin current and to a transverse component in the charge current which corresponds to the anomalous Hall effect.

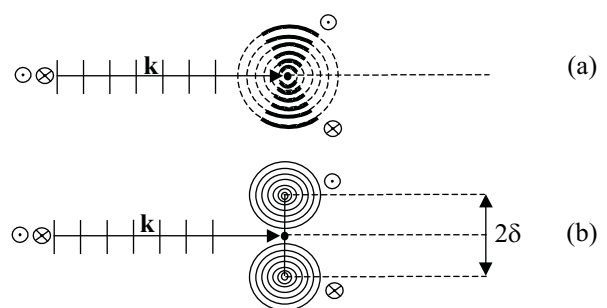


FIG. 1. Schematic picture of the skew-scattering (a) and side-jump (b) mechanisms from a quantum point of view (\odot corresponds to spin up and \otimes to spin down). The bold curves represent the anisotropic enhancement of the amplitude of the wave-packet due to spin-orbit coupling.

The contributions of the skew-scattering and the side-

jump mechanisms to the anomalous Hall resistivity are not similar. For bulk material, it has been shown that, in certain limits, the skew-scattering contribution to the anomalous Hall resistivity is simply proportional to the resistivity^{13,14} while the side-jump contribution is proportional to the square of the resistivity¹⁵. Then, we should have the simple expression

$$\rho_H = \rho_{yx} = a\rho_{xx} + b\rho_{xx}^2, \quad (2)$$

which implies that the relative importance of these two contributions depends both of the temperature and of the impurity concentration. However, we show in this paper that, even if the relation (2) remains correct, the skew-scattering mechanism contributes also to the quadratic term. Such behaviour was already obtained by Kondorskii *et al.*²³.

The traditional way to calculate the anomalous Hall resistivity is to include the contribution of spin-orbit coupling in the transition probability (it leads to the skew-scattering provided one goes beyond the Born approximation) and in the velocity (it leads to the so-called anomalous velocity which gives the side-jump). While the skew-scattering can be obtained in a classical approach it is claimed that the side-jump is a pure quantum effect. We shall discuss this point in the Sec. II of this paper. Most of the calculations of the anomalous Hall resistivity are based on the Boltzmann equation and used severe approximations, in particular concerning the side-jump contribution. Some calculations²³ are based on the Kubo formalism but surprisingly, it is claimed that the side-jump contribution vanishes, and only the skew-scattering contribution is calculated.

Although the anomalous Hall effect is an old phenomena which has motivated a lot of experimental and theoretical studies, a unified model, able to calculate the skew-scattering and side-jump contributions on the same footing, was still missing. In this paper, we propose such model. It is based on the Kubo formalism and have the particularity to be built from the Dirac equation. The choice to use such approach is justified in Sec. III where we discuss in detail the two different approaches of the anomalous Hall effect i.e., based on Dirac and Pauli equations, and study the consistency in the weak-relativistic limit of the expressions of the conductivity tensors obtained in these two approaches. In Sec. IV, we calculated the anomalous Hall resistivity of a disordered ferromagnetic bulk compound. The results, in particular the influence of disorder, are discussed in Sec. V.

II. COMMENTS ON THE PHYSICAL NATURE OF THE SIDE-JUMP MECHANISM

It is often believed that the side-jump is a pure quantum effect and has no classical equivalent. The usual description of the side-jump is then based on a quantum picture (see Fig. 1(b)) of a plane-wave transformed by

scattering in presence of spin-orbit coupling to a spherical wave whose center is shifted in a lateral direction (perpendicular to the momentum and to the spin). The sign of the displacement is opposite for spin up ($s = 1$) and spin down ($s = -1$). A simple calculation in term of phase-shift allows to determine this displacement. We start from the Pauli Hamiltonian

$$H = \frac{p^2}{2m} - \mu_B(\boldsymbol{\sigma} \cdot \mathbf{B}_{eff}) + W, \quad (3)$$

where $\boldsymbol{\sigma}$ is the Pauli matrix, \mathbf{B}_{eff} the exchange field and W the total potential including the spin-orbit coupling

$$W = V + \frac{\hbar}{4m^2c^2}(\boldsymbol{\sigma} \times \nabla V) \cdot \mathbf{p}. \quad (4)$$

We calculate the state $|\Psi_{ks}\rangle$ of the system after scattering given in the Born approximation by the Lippmann-Schwinger equation $|k, s\rangle + \sum_{k's'} |k', s'\rangle G_0(\mathbf{k}', s', \varepsilon_k^s) \langle k', s' | W | k, s \rangle$, where the matrix elements of the potential are

$$\langle k', s' | W | k, s \rangle = \tilde{V}_{\mathbf{k}\mathbf{k}'} \left(\delta_{ss'} + \frac{i\hbar^2}{4m^2c^2} (\boldsymbol{\sigma}_{s's} \times \mathbf{k}') \cdot \mathbf{k} \right). \quad (5)$$

As the spin-orbit term is imaginary, it will influence the phase of the spherical wave. Indeed, for small spin-orbit coupling, the wave function $\Psi_{ks}(\mathbf{r}) = \langle \mathbf{r} | \Psi_{ks} \rangle$ which describes the wave after diffusion can be expressed as

$$\Psi_{ks}(\mathbf{r}) \propto e^{i\mathbf{r} \cdot \mathbf{k}} + \sum_{k'} \delta_{ss'} G_0(\mathbf{k}', s', \varepsilon_k^s) \tilde{V}_{\mathbf{k}\mathbf{k}'} e^{i\mathbf{r}'_s \cdot \mathbf{k}'}, \quad (6)$$

where we have assumed that the effective magnetic field is along the z-direction. The center of the wave packet after scattering is given by

$$\mathbf{r}'_s \equiv \mathbf{r} + \frac{\hbar^2}{4m^2c^2} (\boldsymbol{\sigma}_{ss} \times \mathbf{k}), \quad (7)$$

which is clearly spin dependent and means that the shift of the center of the wave packet is different for spin up and spin down. The lateral displacement, defined as $\boldsymbol{\delta}^s \equiv \mathbf{r}'_s - \mathbf{r}$, is then equal to

$$\boldsymbol{\delta}^s = \frac{\lambda_c}{4mc} (\boldsymbol{\sigma}_{ss} \times \mathbf{p}), \quad (8)$$

where we have introduced the Compton wave length $\lambda_c = \hbar/mc$. Identical expression of $\boldsymbol{\delta}$ was originally derived by Lyo *et al.*²¹. We thus obtain a lateral displacement which is independent of disorder and of order $\lambda_c^2 k_F / 4 \approx 4 \times 10^{-16}$ m i.e., too weak to be consistent with experimental results. However, as it was shown by Berger¹⁵, the band structure effects increase significantly the amplitude by a factor $\alpha \simeq 10^{-4}$ and lead finally to $\delta \approx 10^{-11}$ m.

In a pure classical picture, such a lateral displacement can be experienced by a particle with spin. As a simple example, consider an electron with a charge e ($e < 0$)

subject to an uniform electric field $\mathbf{E} = E\mathbf{u}_x$ ($E > 0$) in the region $x > 0$; there is no field in the region $x < 0$. An incident electron coming from the region $x < 0$ is reflected by the field as sketched in Fig. 2.

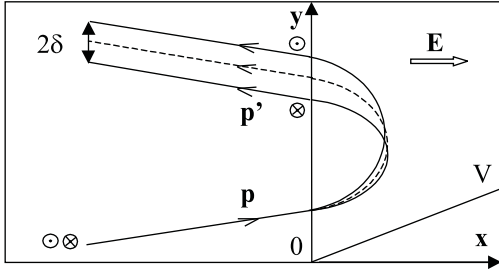


FIG. 2. Classical picture of the side-jump mechanism. The dashed line correspond to the non-relativistic trajectory of the particle and the solids lines to the relativistic trajectories for spin up (\odot) and spin down (\otimes).

The velocity is given by

$$\mathbf{v} = \frac{\partial H}{\partial \mathbf{p}} = \frac{\mathbf{p}}{m} - \frac{e\hbar}{4m^2c^2}(\boldsymbol{\sigma} \times \mathbf{E}), \quad (9)$$

and therefore contains an anomalous contribution $\mathbf{v}_a = -e\hbar(\boldsymbol{\sigma} \times \mathbf{E})/4m^2c^2$ arising from the spin-orbit interaction. In the field region ($x > 0$), where the trajectory is parabolic, the electron (we assume the spin to be along the z-axis) has an anomalous velocity along the y-axis, $v_a^y = -e\hbar(\sigma_z E)/4m^2c^2$. The electron therefore emerges with a shift along y, proportional to its spin σ_z . For an arbitrary electric field, the shift due to the anomalous velocity can be easily calculated

$$\delta = \int_{-\infty}^{+\infty} \mathbf{v}_a dt = - \int_{-\infty}^{+\infty} \frac{e\hbar}{4m^2c^2}(\boldsymbol{\sigma} \times \mathbf{E}) dt, \quad (10)$$

with $e\mathbf{E}dt = d\mathbf{p}$, so that

$$\delta = -\frac{\hbar\boldsymbol{\sigma}}{4m^2c^2} \times \int_{-\infty}^{+\infty} d\mathbf{p} = \frac{\hbar\boldsymbol{\sigma}}{4m^2c^2} \times (\mathbf{p} - \mathbf{p}'), \quad (11)$$

In the above derivation, we have assumed that the spin is perpendicular to the scattering plane. The lateral displacement that we obtain is consistent with the one obtained in the quantum picture. Indeed, the parallel can be simply done by replacing in this classical calculation the momentum by a momentum operator and by making the angular average over the final momentum \mathbf{p}' : thus (11) coincides with (8).

III. COMPARISON OF THE DIRAC AND PAULI APPROACHES

Generally, the calculations of the anomalous Hall resistivity are based on the Pauli Hamiltonian. However, in our modelization, i.e. within the framework of the Kubo

formalism, it appears to be simpler to adopt a relativistic approach based on the Dirac equation. To justify that, let us first remember the derivation of the skew-scattering and the site-jump contributions in the Pauli approach. In presence of an exchange coupling, the Pauli Hamiltonian is $H = \tilde{H} + H_{rc}$ where \tilde{H} is the non-relativistic Hamiltonian

$$\tilde{H} = \frac{p^2}{2m} - \mu_B (\boldsymbol{\sigma} \cdot \mathbf{B}_{eff}) + V, \quad (12)$$

and H_{rc} the first relativistic corrections to the Hamiltonian (order $1/c^2$)

$$H_{rc} = -\frac{p^4}{8m^3c^2} + \frac{\hbar}{4m^2c^2}(\boldsymbol{\sigma} \times \nabla V) \cdot \mathbf{p} + \frac{\hbar^2}{8m^2c^2}\Delta V + H_{rxc}, \quad (13)$$

which contains the relativistic mass corrections, the spin-orbit coupling, the Darwin term and the relativistic corrections to the exchange coupling H_{rxc} . Since the effect we are interested in results from the spin-orbit coupling, we do not need to give the explicit expression of H_{rxc} (calculations and comments on that term are presented in Ref. 33). In this work, we do not consider the contribution of the periodic part of the spin-orbit coupling (i.e., due to the lattice) but only the aperiodic part due to the presence of impurities. In the Pauli approach, the velocity contains two parts. One resulting from the non-relativistic Hamiltonian $\tilde{\mathbf{v}} = \mathbf{p}/m$ and another one resulting from the relativistic corrections

$$\mathbf{v}_{rc} = -\frac{p^2\mathbf{p}}{2m^3c^2} + \frac{\hbar}{4m^2c^2}(\boldsymbol{\sigma} \times \nabla V) + \mathbf{v}_{rxc}. \quad (14)$$

where \mathbf{v}_{rxc} is the velocity related to H_{rxc} . In this description, the spin-orbit contribution to the velocity, the so-called anomalous velocity, appears in a natural and transparent way. When we insert this contribution in the Kubo formula, we obtain the side-jump contribution. It is also possible to isolate the spin-orbit contribution in the Green's function G associated with H by making the following expansion

$$G = \tilde{G} + \tilde{G}H_{rc}\tilde{G} + \tilde{G}H_{rc}\tilde{G}H_{rc}\tilde{G} + \dots, \quad (15)$$

where \tilde{G} is the non-relativistic Green's function associated with the non-relativistic Hamiltonian \tilde{H} . When we report this expression in the Kubo formula and go beyond the Born approximation, we obtain the skew-scattering contribution. Therefore, in the Pauli approach we get separately the skew-scattering and the side-jump contributions when the Green's functions and the velocities are respectively corrected by the spin-orbit coupling.

One important problem in the Pauli approach is to treat disorder. Actually, the spin-orbit coupling introduces two things: off-diagonal disorder (in the tight-binding approximation) and disorder in the velocity

through the anomalous velocity. The second consequence is critical because it is then difficult to calculate precisely the vertex corrections and accordingly the anomalous Hall resistivity. To avoid these problems, we have chosen to based our model on the Dirac equation instead of the Pauli equation. In presence of an exchange coupling, it has the form^{24,25}

$$H = c(\boldsymbol{\alpha} \cdot \mathbf{p}) + \beta mc^2 + V - \mu_B \beta (\boldsymbol{\sigma} \cdot \mathbf{B}_{eff}), \quad (16)$$

where the first term is the kinetic energy, the second term the mass energy, the third term is the potential and the last one the exchange coupling. From (16), we see that the velocity is

$$\mathbf{v} = c\boldsymbol{\alpha} = c \begin{pmatrix} 0 & \boldsymbol{\sigma} \\ \boldsymbol{\sigma} & 0 \end{pmatrix}. \quad (17)$$

A this level, there appears an apparent contradiction between the two approaches since, in the Dirac approach, contrary to the Pauli approach, we do not have any spin-orbit contribution to the velocity (anomalous velocity). It is therefore not clear a priori whether the side-jump mechanism would emerge from the Dirac approach. Actually, in the Dirac approach, the spin-orbit coupling is implicitly taken into account. Therefore, the conductivity should contain simultaneously the skew-scattering and the side-jump contributions as well as higher order contributions in $1/c^2$. However, the expressions of the conductivity obtained in the Dirac and Pauli approaches should coincide in the weak-relativistic limit. To check this, we have calculated, in a formal manner, the weak-relativistic limit up to order $1/c^2$ of the conductivity starting from the Dirac equation and compared it with the conductivity obtained starting from the Pauli equation. The determination of the conductivity tensor is

performed in the Kubo formalism. In certain limits, the conductivity can be expressed like a product of operators, namely Green's functions and velocities. However, the formulations proposed in the literature are often confused or even wrong²⁶⁻²⁸ concerning the off-diagonal elements of the conductivity tensor due to an abusive generalization of the Kubo-Greenwood formula²⁹. In order to clarify the situation, we present in Appendix A the derivation of the conductivity tensor from the original Kubo formula³⁰ and summarize the different stages and approximations which lead first to the Bastin formula³¹ and finally to the Streda formula³². We show that the latter is a sum of two terms, $\tilde{\sigma}_{ij}^I$ and $\tilde{\sigma}_{ij}^{II}$ respectively given, in the limits of independent electrons approximation, zero temperature and zero frequency, by (A15) and (A16)

$$\begin{aligned} \tilde{\sigma}_{ij} &= \tilde{\sigma}_{ij}^I + \tilde{\sigma}_{ij}^{II} \\ &= \frac{e^2 \hbar}{4\pi\Omega} \text{Tr} \langle v_i (G^+ - G^-) v_j G^- - v_i G^+ v_j (G^+ - G^-) \rangle_c \\ &\quad - \frac{e^2}{4i\pi\Omega} \text{Tr} \langle (G^+ - G^-) (r_i v_j - r_j v_i) \rangle_c, \end{aligned} \quad (18)$$

where i and j are the direction indices, Ω the volume of the sample, $\langle \dots \rangle_c$ denotes the average over all the disordered configurations and G^+ and G^- are the retarded and advanced Green's functions at the Fermi level: $G^\pm = G(\varepsilon_F \pm i0) = (\varepsilon_F \pm i0 - H)^{-1}$. The procedure that we have followed is first to report the Dirac velocity and Dirac Green's function in (18), then to perform a weak-relativistic expansion of $\tilde{\sigma}$ and finally to compare it with the expression that we obtain in the Pauli approach. The Dirac velocity is given by (17) and for the Dirac Green's function, we have used an exact expression derived from (16) and given in Ref. 33 by Eq. (A3)

$$G^\pm = \left(\tilde{G}^\pm - \tilde{G}^\pm \frac{\boldsymbol{\sigma} \cdot \mathbf{p}}{2mc} (\varepsilon_F - V - \mu_B (\boldsymbol{\sigma} \cdot \mathbf{B}_{eff})) D^\pm \frac{\boldsymbol{\sigma} \cdot \mathbf{p}}{2mc} \tilde{G}^\pm - \tilde{G}^\pm \frac{\boldsymbol{\sigma} \cdot \mathbf{p}}{2mc} (Q^\pm)^{-1} D^\pm Q^\pm \right) \frac{1}{\frac{1}{2mc^2} D^\pm Q^\pm}, \quad (19)$$

where the operators D^\pm and Q^\pm are given by

$$D^\pm = \left(1 + Q^\pm \frac{(\varepsilon_F - V - \mu_B (\boldsymbol{\sigma} \cdot \mathbf{B}_{eff}))}{2mc^2} \right)^{-1}, \quad (20)$$

$$Q^\pm = 1 + \frac{(\boldsymbol{\sigma} \cdot \mathbf{p}) \tilde{G}^\pm (\boldsymbol{\sigma} \cdot \mathbf{p})}{2m}. \quad (21)$$

The details of the calculations are presented in Appendix B. The determination of the conductivity is done up to order $1/c^2$. It is shown that the identification with the Pauli approach is successful only when one considers the total conductivity $\tilde{\sigma} = \tilde{\sigma}^I + \tilde{\sigma}^{II}$. Indeed, when we compare the expression of $\tilde{\sigma}^I$ obtained in the Dirac approach (see (B6) for order $1/c^0$ and (B11) for order $1/c^2$) to the

one obtained in Pauli approach, we obtained different terms which are exactly canceled by terms in $\tilde{\sigma}^{II}$ (see (B8) for order $1/c^0$ and (B12) for order $1/c^2$). The non-relativistic limit of the total conductivity obtained in the Dirac approach is

$$\begin{aligned} \tilde{\sigma}_{ij}^{(0)} &= \frac{e^2 \hbar}{4\pi\Omega} \text{Tr} \left\langle \frac{p_i}{m} (\tilde{G}^+ - \tilde{G}^-) \frac{p_j}{m} \tilde{G}^- \right. \\ &\quad \left. - \frac{p_i}{m} \tilde{G}^+ + \frac{p_j}{m} (\tilde{G}^+ - \tilde{G}^-) \right\rangle_c \\ &\quad - \frac{e^2}{4i\pi\Omega} \text{Tr} \left\langle (\tilde{G}^+ - \tilde{G}^-) (r_i \frac{p_j}{m} - r_j \frac{p_i}{m}) \right\rangle_c, \end{aligned} \quad (22)$$

which corresponds exactly to the conductivity obtained from (18) when one reports the non-relativistic velocity

$\tilde{\mathbf{v}} = \mathbf{p}/m$ and the non-relativistic Green's function \tilde{G} . The last term in Eq. (22) is zero in absence of external magnetic field. The fact that a supplementary term in $\tilde{\sigma}^{I(0)}$ is present in the Dirac approach and not in the Pauli approach has serious consequences when one neglects $\tilde{\sigma}^{II(0)}$ because it leads to an additional contribution at order $1/c^0$ to the off-diagonal conductivity which does not disappear in the non-relativistic limit and thus would give unphysical results. At order $1/c^2$, the total conductivity obtained in the Dirac approach is

$$\tilde{\sigma}_{ij}^{(2)} = \tilde{\sigma}_{ij}^{SS} + \tilde{\sigma}_{ij}^{SJ} + \tilde{\sigma}_{ij}^{or}, \quad (23)$$

where $\tilde{\sigma}_{ij}^{SS}$ contains the terms which lead to the skew-scattering

$$\begin{aligned} \tilde{\sigma}_{ij}^{SS} = & \frac{e^2 \hbar}{4\pi\Omega} \text{Tr} \left\langle \frac{p_i}{m} (\tilde{G}^+ H_{rc} \tilde{G}^+ - \tilde{G}^- H_{rc} \tilde{G}^-) \frac{p_j}{m} \tilde{G}^- \right. \\ & + \frac{p_i}{m} (\tilde{G}^+ - \tilde{G}^-) \frac{p_j}{m} \tilde{G}^- H_{rc} \tilde{G}^- \\ & - \frac{p_i}{m} \tilde{G}^+ H_{rc} \tilde{G}^+ \frac{p_j}{m} (\tilde{G}^+ - \tilde{G}^-) \\ & \left. - \frac{p_i}{m} \tilde{G}^+ \frac{p_j}{m} (\tilde{G}^+ H_{rc} \tilde{G}^+ - \tilde{G}^- H_{rc} \tilde{G}^-) \right\rangle_c. \quad (24) \end{aligned}$$

$\tilde{\sigma}_{ij}^{SJ}$ contains the terms which lead to the side-jump

$$\begin{aligned} \tilde{\sigma}_{ij}^{SJ} = & \frac{e^2 \hbar}{4\pi\Omega} \text{Tr} \left\langle (\mathbf{v}_{rc})_i (\tilde{G}^+ - \tilde{G}^-) \frac{p_j}{m} \tilde{G}^- \right. \\ & - (\mathbf{v}_{rc})_i \tilde{G}^+ \frac{p_j}{m} (\tilde{G}^+ - \tilde{G}^-) + \frac{p_i}{m} (\tilde{G}^+ - \tilde{G}^-) (\mathbf{v}_{rc})_j \tilde{G}^- \\ & \left. - \frac{p_i}{m} \tilde{G}^+ (\mathbf{v}_{rc})_j (\tilde{G}^+ - \tilde{G}^-) \right\rangle, \quad (25) \end{aligned}$$

and $\tilde{\sigma}_{ij}^{or}$ is equal to

$$\begin{aligned} \tilde{\sigma}_{ij}^{or} = & -\frac{e^2}{4i\pi\Omega} \text{Tr} \left\langle (\tilde{G}^+ - \tilde{G}^-) (r_i (\mathbf{v}_{rc})_j - r_j (\mathbf{v}_{rc})_i) \right. \\ & \left. + (\tilde{G}^+ H_{rc} \tilde{G}^+ - \tilde{G}^- H_{rc} \tilde{G}^-) \left(r_i \frac{p_j}{m} - r_j \frac{p_i}{m} \right) \right\rangle_c. \quad (26) \end{aligned}$$

In addition to the skew-scattering and the side-jump contributions to the anomalous Hall effect, we identify a new contribution, $\tilde{\sigma}_{ij}^{or}$, which is related to the orbital momentum $\mathbf{L} = \mathbf{r} \times \mathbf{p}$. The expression (23) of the conductivity corresponds exactly to the one which is obtained from (18) when one reports the first order correction to the velocity \mathbf{v}_{rc} and the the first order correction to the Green function $\tilde{G} H_{rc} \tilde{G}$ where \mathbf{v}_{rc} and H_{rc} are given respectively by Eqs. (13) and (14). We have then proved in the weak-relativistic limit (up to order $1/c^2$) the coincidence of the conductivity in the two approaches.

In summary, from the Pauli Hamiltonian, we get the skew-scattering and the side-jump contributions separately while, from the Dirac Hamiltonian, we get the both contributions and also higher order with $1/c^2$ contributions simultaneously. Therefore, in a full relativistic Dirac description, it will be difficult to quantify the importance of each contributions. However, this approach

has a great advantage over the Pauli approach: it allows a simpler treatment of disordered material because, contrary to the Pauli approach where both the velocities and the Green's functions contain disorder, the disorder is only present in the Green's functions. It is thus possible to put one of the velocity operator outside of the average over disordered configurations and to calculate precisely the vertex corrections to the conductivity. For this reason, the Dirac approach is more efficient to calculate the anomalous Hall resistivity.

In the next section, we present a direct application of our model. In order to perform the analytical calculations, we have restricted ourselves to the weak-relativistic limit and approximated calculations of the vertex corrections; then the results that we obtain can still be compared to the one obtained in the Pauli approach.

IV. ANOMALOUS HALL RESISTIVITY OF A DISORDERED FERROMAGNETIC COMPOUND

In this section, we present the calculation of the anomalous Hall resistivity of a disordered ferromagnetic bulk compound. This calculation is done in both Dirac and Pauli models in order to show the similarities and the differences between these two approaches. We consider a system with a cubic symmetry and a magnetization along the z-axis. For such system, the Casimir-Onsager conditions for the conductivity tensor yield to the following symmetry

$$\tilde{\sigma} = \begin{pmatrix} \tilde{\sigma}_{xx} & \tilde{\sigma}_{xy} & 0 \\ -\tilde{\sigma}_{xy} & \tilde{\sigma}_{xx} & 0 \\ 0 & 0 & \tilde{\sigma}_{zz} \end{pmatrix}. \quad (27)$$

We are only interested by the relativistic corrections to the off-diagonal elements which correspond to the anomalous Hall effect. We do not study the relativistic corrections to the diagonal elements which correspond to the anisotropic magneto-resistance (AMR) and lead to a difference of order $1/c^4$ between $\tilde{\sigma}_{xx}$ and $\tilde{\sigma}_{zz}$. Thus, in this work, the diagonal elements are calculated to order $1/c^0$ and by consequence are all equal, while the off-diagonal elements are calculated to order $1/c^2$. To get analytical expressions, we have made several approximations: free-electron approximation, weak-disorder limit and weak-relativistic limit for the Dirac approach. We are interested with the residual resistivity which result from the presence of disorder, then the conductivity is the sum of $\tilde{\sigma}^I$ given by (A15) and of $\tilde{\sigma}^{II}$ given by (A16)

$$\begin{aligned} \tilde{\sigma}_{ij} = & \frac{e^2 \hbar}{4\pi\Omega} \text{Tr} \langle v_i (G^+ - G^-) v_j G^- \\ & - v_i G^+ v_j (G^+ - G^-) \rangle_c \\ & - \frac{e^2}{4i\pi\Omega} \text{Tr} \langle (G^+ - G^-) (r_i v_j - r_j v_i) \rangle_c, \quad (28) \end{aligned}$$

where the Green's function G^\pm is associated with the total Hamiltonian: $G^\pm = (\varepsilon_F \pm i0 - H)^{-1} = (\varepsilon_F \pm i0 -$

$H_0 - W)^{-1}$ where H_0 is the non-disordered Hamiltonian and W the perturbation (equal to the potential V in the Dirac approach and to $V + H_{so}$ in the Pauli approach where H_{so} is the spin-orbit coupling). We modelize the compound in this way: the total volume of the sample $\Omega = L^3$ is divided in N cells of volume $\Omega_0 = a^3$. In each cell, the potential takes a constant value V with a probability distribution $P(V)$ which is characterized by its moments $\langle V^n \rangle_c = \int P(V) V^n dV$. A proper choice of the energy origin gives $\langle V \rangle = 0$. We assume that there are not correlations in the value of the potential in different cells. In this first approach, we neglect in (28) the

contribution of the terms which involves product of two advanced (or retarded) Green's functions. Such approximation is justified in the weak-disorder limit³⁴. In Appendix B, we have shown that $\tilde{\sigma}^{II}$, calculated in the Dirac approach, contains two parts, the first one related to the orbital momentum, which is negligible in our model, and the second one which is exactly compensated by terms in $\tilde{\sigma}^I$. Then, we do not need to calculate this contribution. The conductivity reduces to

$$\tilde{\sigma}_{ij} = \frac{e^2 \hbar}{2\pi\Omega} \text{Tr} \langle v_i G^+ v_j G^- \rangle_c. \quad (29)$$

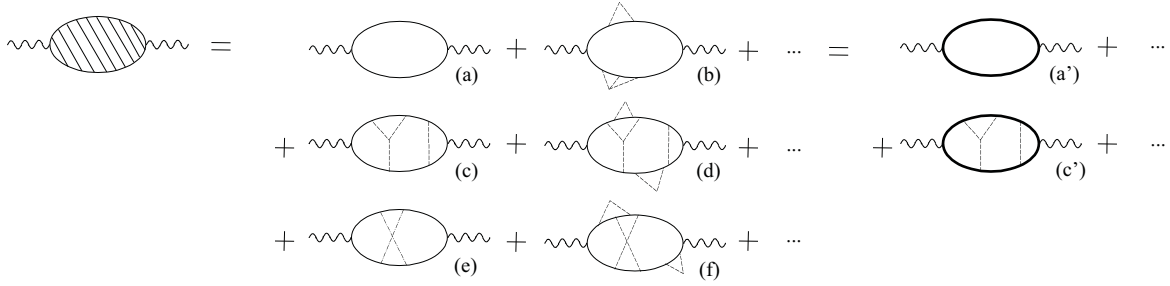


FIG. 3. Illustration of the conductivity with the help of Feymann diagrams. The total conductivity (hatched diagram), expressed like an infinite sum of diagrams involving the non-disordered Green's function G_0 (thin curve line), can be rewrite like an infinite sum of diagrams involving the average Green's function \underline{G} (bold curve line). The wave lines refer to the velocity and the dashed lines to the potential.

We introduce first the t-matrix $T = W + W G_0 T$ which allows to write the Green's function as $G = G_0 + G_0 T G_0$ where G_0 is the non-disordered Green's function. Reporting this in (29), we get

$$\tilde{\sigma}_{ij} = \frac{e^2 \hbar}{2\pi\Omega} \text{Tr} \langle v_i G_0^+ v_j G_0^- \rangle_c + \frac{e^2 \hbar}{2\pi\Omega} \text{Tr} \langle v_i G_0^+ T G_0^+ v_j G_0^- T G_0^- \rangle_c. \quad (30)$$

This equation can be illustrate with the help of Feymann diagrams as is done on the Fig. 3. The conductivity $\tilde{\sigma}_{ij}$, represented by the full diagram, is then express as a sum of an infinite number of diagrams. Only few of them are depicted on Fig. 3: diagram (a) which corresponds to the first term in (30) and diagrams from (b) to (f) which are some representative samples of the kind of diagrams which give the second term in (30). The main approximation done in our calculation is to neglect the crossed diagrams which correspond to weak-localization corrections, i.e., we neglect diagrams such (e) and (f) and we keep only the so-called ladder diagrams. Weak-localization corrections to the anomalous Hall resistivity will be discussed in a separate paper. We introduce the configuration averaged Green's function $\underline{G} = \langle G \rangle_c$ which can be written with the help of

the self-energy $\Sigma = \langle W G_0 W \rangle_c + \langle W G_0 W G_0 W \rangle_c + \dots$ as $\underline{G} = (\varepsilon_F - H_0 - \Sigma)^{-1}$. When we neglect the crossed diagrams, (30) can be written as

$$\tilde{\sigma}_{ij} \equiv \tilde{\sigma}_{ij}^{bubble} + \tilde{\sigma}_{ij}^{vertex} = \frac{e^2 \hbar}{2\pi\Omega} \text{Tr} \langle v_i \underline{G}^+ v_j \underline{G}^- \rangle_c + \frac{e^2 \hbar}{2\pi\Omega} \text{Tr} \langle v_i \underline{G}^+ T' \underline{G}^+ v_j \underline{G}^- T' \underline{G}^- \rangle_c, \quad (31)$$

with T' solution of $T' = W + W \underline{G} T'$. The first term in the right side hand is the so-called bubble term and the second one corresponds to the vertex corrections. Within this transformation, the calculation of the conductivity is then reduced to two distinct problems: determination of the average Green's function (i.e., the self-energy) and calculation of the vertex corrections. Because of the weak-disorder limit, we keep in the self-energy and the t-matrix the lowest sufficient orders

$$\begin{cases} \Sigma = \langle W G_0 W \rangle_c \\ T' = W + W \underline{G} W \end{cases}. \quad (32)$$

In the t-matrix, we have to keep the terms up to the second order with V because it is necessary to go beyond the Born approximation to get the skew-scattering. The

explicit calculation of (31) in the approximations (32) for the Dirac and Pauli approaches is presented in the next two sections.

A. Dirac approach

We assume free electrons in a uniform exchange field \mathbf{B}_{eff} aligns along the z-axis and submitted to a disordered potential. The non-perturbed part of the Hamiltonian is

$$H_0 = c(\boldsymbol{\alpha} \cdot \mathbf{p}) + (\beta - 1)mc^2 - \mu_B \beta \sigma_z B_{eff}, \quad (33)$$

and the perturbation part is simply the potential $W = V$. The matrix elements of the average Green's function are $\langle k, s | \underline{G}^\pm | k, s \rangle = (\varepsilon_F - \varepsilon_k^s \pm i\hbar/2\tau_k^s)^{-1}$ where the eigenvalues ε_k^s of (33) are in the weak-relativistic limit equals to

$$\varepsilon_k^s = \frac{\hbar^2 k^2}{2m} - s\mu_B B_{eff} + o\left(\frac{1}{c^2}\right), \quad (34)$$

for the upper band, and

$$\varepsilon_{\underline{k}}^s = -2mc^2 + o\left(\frac{1}{c^0}\right), \quad (35)$$

for the lower band. The s index refers to the spin ($s = 1$ for spin up and $s = -1$ for spin down), the k index refers to the upper band and the \underline{k} to the lower band. The lifetime τ_k^s which appears in the expression of the average Green's function is given by

$$\begin{aligned} \frac{\hbar}{2\tau_k^s} &= -\text{Im}\langle k, s | \Sigma | k, s \rangle = -\text{Im}\langle k, s | \langle V G_0 V \rangle_c | k, s \rangle \\ &= \pi \Omega_0 \mathcal{N}_s(\varepsilon_k^s) \langle V^2 \rangle_c, \end{aligned} \quad (36)$$

where \mathcal{N}_s is the density of states of spin s by unit volume. In the Dirac model, the velocity \mathbf{v} is simply equal to $c\boldsymbol{\alpha}$. Because we have chosen to work in the basis where the non-perturbed Hamiltonian H_0 (and by consequence the Green's function G_0) is diagonal, we have to calculate the velocity in this basis, we get

$$\mathbf{v} = \begin{pmatrix} \mathbf{u}(\mathbf{k}) + o\left(\frac{1}{c^2}\right) & c\boldsymbol{\sigma} + o\left(\frac{1}{c}\right) \\ c\boldsymbol{\sigma} + o\left(\frac{1}{c}\right) & o(c^0) \end{pmatrix}, \quad (37)$$

where $\mathbf{u}(\mathbf{k})$ is the (2×2) matrix

$$\mathbf{u}(\mathbf{k}) = \frac{\hbar \mathbf{k}}{m} \begin{pmatrix} 1 & 0 \\ 0 & 1 \end{pmatrix}. \quad (38)$$

We have now all the ingredients to calculate the bubble term in (31)

$$\begin{aligned} \tilde{\sigma}_{ij}^{bubble} &= \frac{e^2 \hbar}{2\pi \Omega} \sum_{kss'} \langle k, s | v_i | k, s' \rangle \langle k, s' | \underline{G}^+ | k, s' \rangle \\ &\times \langle k, s' | v_j | k, s \rangle \langle k, s | \underline{G}^- | k, s \rangle. \end{aligned} \quad (39)$$

The average over the disordered configurations $\langle \dots \rangle_c$ has been dropped because in the Dirac approach the velocity is a non-disordered quantity. At order $1/c^0$, only the diagonal elements ($s = s'$, no spin-flip) of the velocity and the particles in the upper band contribute, then we have

$$\tilde{\sigma}_{ij}^{bubble} = \frac{e^2 \hbar^3}{2\pi m^2 \Omega} \sum_{ks} \frac{k_i k_j}{(\varepsilon_F - \varepsilon_k^s)^2 + \frac{\hbar^2}{4(\tau_k^s)^2}}. \quad (40)$$

The dispersion law ε_k^s given by (34) is isotropic at order $1/c^0$. Then, the angular dependence is entirely contained in the factor $k_i k_j$, which means that only diagonal components of the conductivity are different from zero. As we consider the lowest order contribution with V , we do not need to calculate the vertex corrections to the diagonal components, the total conductivity $\tilde{\sigma}_{ii}$ is then approximated by $\tilde{\sigma}_{ii}^{bubble}$. After integration over k , we get

$$\tilde{\sigma}_{xx} = e^2 \mathcal{N}_\uparrow \frac{l^\uparrow v_F^\uparrow}{3} + e^2 \mathcal{N}_\downarrow \frac{l^\downarrow v_F^\downarrow}{3} \equiv \tilde{\sigma}_{xx}^\uparrow + \tilde{\sigma}_{xx}^\downarrow, \quad (41)$$

which corresponds to the Einstein relation with two spin channels where $l^s = v_F^s \tau_F^s$ is the mean-free-path, v_F^s and \mathcal{N}_s are respectively the velocity and the density of states by unit volume at the Fermi energy for spin s (identical expressions are obtained for $\tilde{\sigma}_{yy}$ and $\tilde{\sigma}_{zz}$). The diagram which gives this contribution is depicted on figure 4.



FIG. 4. Bubble diagram contributing to the diagonal conductivity $\tilde{\sigma}_{xx}$. The signs $+/-$ refer to the retarded/advanced average Green's function \underline{G}^\pm .

The off-diagonal components of the conductivity arise only when we take the vertex corrections into account. If we expand the t-matrix up to the second order in V , from (31), we get

$$\begin{aligned} \tilde{\sigma}_{ij}^{vertex} &= \frac{e^2 \hbar}{2\pi \Omega} \text{Tr} \langle v_i \underline{G}^+ (V + V \underline{G}^+ V) \underline{G}^+ \\ &\times v_j \underline{G}^- (V + V \underline{G}^- V) \underline{G}^- \rangle_c. \end{aligned} \quad (42)$$

We then need the potential in the new basis

$$V = \tilde{V}(\mathbf{k}' - \mathbf{k}) \begin{pmatrix} U(\mathbf{k}, \mathbf{k}') + o\left(\frac{1}{c^4}\right) & \frac{\hbar(\boldsymbol{\sigma} \cdot \mathbf{k}')}{2mc} + o\left(\frac{1}{c^3}\right) \\ \frac{\hbar(\boldsymbol{\sigma} \cdot \mathbf{k}')}{2mc} + o\left(\frac{1}{c^3}\right) & o(c^0) \end{pmatrix}, \quad (43)$$

where $U(\mathbf{k}, \mathbf{k}')$ is the (2×2) matrix

$$U(\mathbf{k}, \mathbf{k}') = \left(\frac{1 - \frac{\hbar^2((\mathbf{k}' - \mathbf{k})^2 + 2i(\mathbf{k}' \times \mathbf{k}) \cdot \mathbf{e}_z)}{8m^2c^2}}{\hbar^2((k'_x + ik'_y)k'_z - (k_x + ik_y)k_z - i(\mathbf{k}' \times \mathbf{k}) \cdot (\mathbf{e}_x + i\mathbf{e}_y))} \frac{\hbar^2((k'_x - ik'_y)k'_z - (k_x - ik_y)k_z - i(\mathbf{k}' \times \mathbf{k}) \cdot (\mathbf{e}_x - i\mathbf{e}_y))}{4m^2c^2} \right), \quad (44)$$

and $\tilde{V}(\mathbf{q}) = \int d\mathbf{r} e^{i\mathbf{q} \cdot \mathbf{r}} V(\mathbf{r}) / \Omega$ is the Fourier transform of the potential. When we study in detail all the diagrams contain in (42), we see that only two kind of diagrams³⁵ contribute to the conductivity at order $1/c^2$. These diagrams are depicted on figures 5 and 6 (left column).

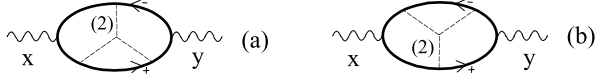


FIG. 5. Diagrams contributing to the off-diagonal conductivity $\tilde{\sigma}_{xy}$ through the skew-scattering mechanism in both Pauli and Dirac approaches. The number in bracket indicates the order with $1/c$ of the matrix elements of the velocity (wave line), average Green's function (bold curve line) and potential (dashed line). It is omitted in case of zero order with $1/c$.

The first series of diagrams (see Fig. 5) involves velocities at order $1/c^0$, Green's functions at order $1/c^0$, which means that only particles in the upper band contribute, and potential twice at order $1/c^0$ and once at order $1/c^2$ which ensures a total order of $1/c^2$ for the conductivity. The diagrams of this first series correspond to the skew-scattering mechanism. The second series of diagrams (left column on Fig. 6) involves one velocity at order $1/c^0$ and one at order c , three Green's functions at order $1/c^0$ and one at order $1/c^2$, which means that we have a transition of particles between the upper and lower bands, and potential one time at order $1/c^0$ and one time at order $1/c$ which ensures a total order of $1/c^2$ for the conductivity. The diagrams of this second series correspond to the side-jump mechanism. In the following, we present the explicit calculation of the conductivity due to these two series. Let us start with the skew-scattering. We present the calculation of the diagram (a) on Fig. 5, which gives

$$\begin{aligned} \tilde{\sigma}_{xy}^{(5a)} &= \frac{e^2 \hbar}{2\pi\Omega} \sum_{kk'k''s} \left\langle \langle k, s | v_x | k, s \rangle^{(0)} \langle k, s | \underline{G}^+ | k, s \rangle^{(0)} \right. \\ &\times \langle k, s | V | k', s \rangle^{(0)} \langle k', s | \underline{G}^+ | k', s \rangle^{(0)} \langle k', s | V | k'', s \rangle^{(0)} \\ &\times \langle k'', s | \underline{G}^+ | k'', s \rangle^{(0)} \langle k'', s | v_y | k'', s \rangle^{(0)} \langle k'', s | \underline{G}^- | k'', s \rangle^{(0)} \\ &\times \left. \langle k'', s | V | k, s \rangle^{(2)} \langle k, s | \underline{G}^- | k, s \rangle^{(0)} \right\rangle_c. \end{aligned} \quad (45)$$

The number in bracket indicates the order with $1/c$ of the matrix elements like in Fig. 5 when the order is different from zero. We remark that for a total order $1/c^2$ of the conductivity, the spin is conserved during the process (no spin-flip scattering). We report in this expression, the matrix elements given by (38) and (44) and perform the integration over k , k' and k'' . The final expression of the conductivity due to the diagram (a) is a com-

plex quantity. The calculation of the diagram (b) gives the conjugated expression, then the total contribution due to the skew-scattering mechanism is a real quantity equal to

$$\begin{aligned} \tilde{\sigma}_{xy}^{SS} &= -\frac{\pi}{6} \frac{\langle V^3 \rangle_c}{\langle V^2 \rangle_c} \left(\mathcal{N}_\uparrow \Omega_0 \tilde{\sigma}_{xx}^\uparrow \left(\frac{v_F^\uparrow}{c} \right)^2 - \mathcal{N}_\downarrow \Omega_0 \tilde{\sigma}_{xx}^\downarrow \left(\frac{v_F^\downarrow}{c} \right)^2 \right) \\ &\equiv \tilde{\sigma}_{xy}^{SS\uparrow} + \tilde{\sigma}_{xy}^{SS\downarrow}. \end{aligned} \quad (46)$$

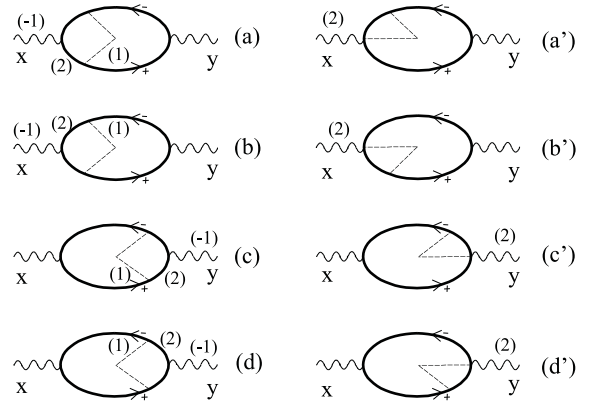


FIG. 6. Diagrams contributing to the off-diagonal conductivity $\tilde{\sigma}_{xy}$ through the side-jump mechanism in Dirac approach (left column) and Pauli approach (right column). The number in bracket indicates the order with $1/c$ of the matrix elements of the velocity (wave line), average Green's function (bold curve line) and potential (dashed line).

We turn now our interest to the side-jump mechanism. The diagram (a) of Fig. 6 gives

$$\begin{aligned} \tilde{\sigma}_{xy}^{(6a)} &= \frac{e^2 \hbar}{2\pi\Omega} \sum_{kk's} \left\langle \langle k, s | v_x | k, s \rangle^{(-1)} \langle k, s | \underline{G}^+ | k, s \rangle^{(2)} \right. \\ &\times \langle k, s | V | k', s \rangle^{(1)} \langle k', s | \underline{G}^+ | k', s \rangle^{(0)} \langle k', s | v_y | k', s \rangle^{(0)} \\ &\times \left. \langle k', s | \underline{G}^- | k', s \rangle^{(0)} \langle k', s | V | k, s \rangle^{(0)} \langle k, s | \underline{G}^- | k, s \rangle^{(0)} \right\rangle_c. \end{aligned} \quad (47)$$

In this mechanism, due to the presence of off-diagonal elements in the velocity (37) and the potential (43), a particle of the upper band ε_k^s experiences a virtual transition in the lower band ε_k^- associated to the opposite spin. We perform the integrations over k and k' , add the contributions of the four diagrams of the Fig. 6 and finally obtained

$$\tilde{\sigma}_{xy}^{SJ} = -e^2 \mathcal{N}_\uparrow \frac{2\delta^\uparrow v_F^\uparrow}{3} + e^2 \mathcal{N}_\downarrow \frac{2\delta^\downarrow v_F^\downarrow}{3} \equiv \tilde{\sigma}_{xy}^{SJ\uparrow} + \tilde{\sigma}_{xy}^{SJ\downarrow}, \quad (48)$$

where δ^s is the transverse displacement (or side-jump) given by $\hbar v_F^s/4mc^2 = \lambda_c^2 k_F^s/4$. The expression of $\tilde{\sigma}_{xy}$ for the side-jump is similar to the expression (41) of $\tilde{\sigma}_{xx}$ but instead of the mean-free-path l , we have 2δ . In contrast to $\tilde{\sigma}_{xy}^{SS}$, the side-jump contribution to the off-diagonal conductivity is independent of disorder.

B. Pauli approach

In the Pauli approach, the Hamiltonian given by (3) is the sum of a non-perturbed part and a perturbation V given by (4) which contains the potential and the spin-orbit coupling. The velocity associated with this Hamiltonian consists of a normal part and an anomalous part due to the spin-orbit coupling

$$\mathbf{v} = \frac{\mathbf{p}}{m} + \frac{\hbar}{4m^2c^2} (\boldsymbol{\sigma} \times \nabla V). \quad (49)$$

We neglect the contribution of the spin-orbit coupling in the life-time, then the average Green's function is $\underline{G}^\pm = (\varepsilon_F - H_0 \mp i\hbar/\tau_k^s)^{-1}$ where τ_k^s is given by (36). Because of this approximation, the derivation of the diagonal conductivity $\tilde{\sigma}_{xx}$ is similar to one done in the Dirac approach and we obtain the expression (41).

The off-diagonal elements of the conductivity are obtained from the vertex corrections. For the skew-scattering, the diagrams which contribute are exactly the same than in the Dirac approach (see Fig. 5) because the only terms in the potential (44) which contribute in the Dirac approach correspond precisely to the potential in the Pauli approach which is

$$\langle k, s | W | k', s' \rangle = \tilde{V}(\mathbf{k}' - \mathbf{k}) \left(1 + \frac{i\hbar^2}{4m^2c^2} \boldsymbol{\sigma}_{ss'} \cdot (\mathbf{k} \times \mathbf{k}') \right). \quad (50)$$

The other terms in (44) are Darwin-like terms and do not contribute to the off-diagonal conductivity. Then, in the Pauli approach, the skew-scattering mechanism corresponds to the same Feynman diagrams and gives the same final expression (46) as the weak-relativistic limit of the Dirac approach.

Concerning the side-jump, the correspondence between the two approaches is not so simple. In the Dirac approach, we have seen that a virtual transition occurs from the upper band to the lower band. In the Pauli approach, no such transition can take place because there is only one band. However, we have a supplementary part in the velocity, the anomalous velocity which is of order $1/c^2$ and leads to the side-jump mechanism. The corresponding diagrams are depicted on the right column of Fig. 6. For each diagram in the left column (i.e. in the Dirac approach), we have an equivalent diagram in the right column (i.e. in the Pauli approach). The change between the left and right column corresponds to a vertex

renormalization because the matrix elements of the product $\mathbf{v}GV$ in the Dirac approach are equal to the matrix elements of \mathbf{v} in the Pauli approach

$$\begin{aligned} \langle k, s | \mathbf{v} | k', s' \rangle &= \frac{\hbar \mathbf{k}}{m} \delta_{kk'} \delta_{ss'} \\ &+ \tilde{V}(\mathbf{k}' - \mathbf{k}) \frac{i\hbar}{4m^2c^2} \boldsymbol{\sigma}_{ss'} \times (\mathbf{k} - \mathbf{k}'). \end{aligned} \quad (51)$$

Thus, when we calculate, for example the diagram (6a')

$$\begin{aligned} \tilde{\sigma}_{xy}^{(6a')} &= \frac{e^2 \hbar}{2\pi\Omega} \sum_{kk's} \left\langle \langle k, s | v_x | k', s \rangle^{(2)} \langle k', s | \underline{G}^+ | k', s \rangle^{(0)} \right. \\ &\times \langle k', s | v_y | k', s \rangle^{(0)} \langle k', s | \underline{G}^- | k', s \rangle^{(0)} \\ &\times \left. \langle k', s | V | k, s \rangle^{(0)} \langle k, s | \underline{G}^- | k, s \rangle^{(0)} \right\rangle_c, \end{aligned} \quad (52)$$

we obtain the same contribution than from the expression (47) of the diagram (6a). The final result, after summation over the four diagrams (6a') to (6d'), is then identical to (48).

V. DISCUSSION

We want now to discuss briefly the influence of disorder on the resistivity and on the anomalous Hall resistivity which are, in the limit $\tilde{\sigma}_{xy} \ll \tilde{\sigma}_{xx}$, simply given by $\tilde{\rho}_{xx} \simeq 1/\tilde{\sigma}_{xx}$ and $\tilde{\rho}_H = -\tilde{\rho}_{xy} \simeq \tilde{\sigma}_{xy}/\tilde{\sigma}_{xx}^2$. The only terms which depend of disorder in the expressions of $\tilde{\sigma}_{xy}$ given by (46) and (48) and of $\tilde{\sigma}_{xx}$ given by (41), are the moments $\langle V^2 \rangle_c$ and $\langle V^3 \rangle_c$. Indeed, we have

$$\begin{cases} \tilde{\sigma}_{xx} \propto \frac{1}{\langle V^2 \rangle_c} \\ \tilde{\sigma}_{xy}^{SS} \propto \frac{\langle V^3 \rangle_c}{\langle V^2 \rangle_c^2} \\ \tilde{\sigma}_{xy}^{SJ} \text{ indep. of disorder} \end{cases}. \quad (53)$$

Then, the variations with disorder of the resistivity and the anomalous Hall resistivity are like $\tilde{\rho}_{xx} \propto \langle V^2 \rangle_c$, $\tilde{\rho}_{xy}^{SS} \propto \langle V^3 \rangle_c$ and $\tilde{\rho}_{xy}^{SJ} \propto \langle V^2 \rangle_c^2$. To illustrate this dependence, we consider a binary alloy $A_x B_{1-x}$ for which

$$\langle V^2 \rangle_c = x(1-x)(\varepsilon_A - \varepsilon_B)^2, \quad (54)$$

and,

$$\langle V^3 \rangle_c = x(1-x)(1-2x)(\varepsilon_A - \varepsilon_B)^3, \quad (55)$$

where $\varepsilon_{A(B)}$ is the value that the potential V takes on site $A(B)$ and x is the concentration of sites A . Keeping the lowest orders in x (weak-disorder limit), we get

$$\begin{cases} \tilde{\rho}_{xx} \propto x \\ \tilde{\rho}_{xy}^{SS} \propto (x - 3x^2) \\ \tilde{\rho}_{xy}^{SJ} \propto x^2 \end{cases}, \quad (56)$$

which is in agreement with the simple relation given by (2) but in contradiction with the common belief that the quadratic term would arise only from the side-jump mechanism. In fact, the skew-scattering mechanism,

which is responsible for the linear term, gives also an important contribution to the quadratic term. Such result was already obtained by Kondorskii *et al.*²³. In addition, our calculations precise all the approximations which founded the relation (2) and shows that it should not be valid in the general case, in particular for high disordered system, high relativistic limit, complex band structure or in the case of heterogeneous systems such as thin films or multilayers.

The Hall angle, which corresponds to the angle between the electric field and the charge current, is an interesting quantity. For an applied electric field in the x-direction and an effective magnetic field in the z-direction, we have: $\text{tg}(\theta_H) \equiv j_y/j_x = \tilde{\sigma}_{yx}/\tilde{\sigma}_{xx}$. The conductivity elements $\tilde{\sigma}_{xx}$ and $\tilde{\sigma}_{yx}$ are in a first approximation the sums of contributions due to spins up and down. We can thus define a spin-dependent Hall angle

$$\text{tg}(\theta_H^{\uparrow(1)}) \equiv \frac{j_y^{\uparrow(1)}}{j_x^{\uparrow(1)}} = \frac{\tilde{\sigma}_{yx}^{\uparrow(1)}}{\tilde{\sigma}_{xx}^{\uparrow(1)}}. \quad (57)$$

We report the expressions (46) and (48) of the skew-scattering and side-jump off-diagonal conductivities as well as the expression (41) of the diagonal conductivity and obtain for spin s

$$\theta_H^s \approx s \left(\frac{2\delta^s}{l^s} + \frac{\pi}{6} \frac{\langle V^3 \rangle_c}{\langle V^2 \rangle_c} \mathcal{N}_s \Omega_0 \left(\frac{v_F^s}{c} \right)^2 \right). \quad (58)$$

θ_H^\uparrow and θ_H^\downarrow are not only opposite in sign, they take distinct absolute values due to spin polarization. As a consequence, the charge current ($\mathbf{j}^\uparrow + \mathbf{j}^\downarrow$) has a non-zero transverse component and the spin current ($\mathbf{j}^\uparrow - \mathbf{j}^\downarrow$) has a non-zero longitudinal component. The magnitude of the Hall angle is determined in the weak-disorder limit

APPENDIX A: FROM THE KUBO FORMULA TO THE STREDA FORMULA

In the linear response approximation, Kubo has shown that the conductivity tensor is related to a two currents correlation function³⁰

$$\tilde{\sigma}_{ij}(\omega) = \Omega \lim_{s \rightarrow 0^+} \int_0^\beta d\lambda \int_0^{+\infty} dt e^{\frac{i\hbar}{\hbar}(-\hbar\omega + is)} \times \text{Tr} \left\langle \rho_0 J_j(0) J_i(t + i\hbar\lambda) \right\rangle_c, \quad (A1)$$

where it is assumed that the applied field leads to a time-dependent perturbation of the form: $H'(t) = H'_0 \exp(\frac{i\hbar}{\hbar}(-\hbar\omega + is))$. Ω is the volume of the sample, β is

mostly by the skew-scattering contribution. Indeed, in this limit we have $\theta_H^{S,J} \approx 2\delta/l \approx 10^{-3}$ whereas $\theta_H^{S,S} \approx \pi(1-2x)(\varepsilon_A - \varepsilon_B)\varepsilon_F/3mc^2W \approx 5.10^{-2}$ where we have taken $l \approx 200$ Å, $x \approx 0.2$, $\varepsilon_A - \varepsilon_B \approx 2$ eV, $\varepsilon_F \approx 10$ eV, the band width $W \approx 5$ eV, $mc^2 \simeq 500$ keV and a band factor $\alpha \approx 10^4$. For simplicity, we have dropped the spin index. This order of magnitude is consistent with experimental results²². When the disorder increases, the mean-free-path l decreases significantly which means, as the quantity δ is disorder independent, an increase of the side-jump contribution to the Hall angle. However, the skew-scattering contribution to the Hall angle increases on the same way. It is thus not possible to predict in this first approach which contribution is dominant in the high disorder regime.

To summarize, we have, in this article, proposed a model based on the Dirac equation and on the Kubo formalism which allows to calculate on the same footing the anomalous Hall resistivity due to both skew-scattering and side-jump mechanisms. The consistence of this approach with the one based on the Pauli equation has been studied in detail in the weak-relativistic limit. In particular, we have shown that in order to calculate the anomalous Hall conductivity one has to consider in the Dirac approach the total conductivity $\tilde{\sigma}^I + \tilde{\sigma}^{II}$, otherwise unphysical results are obtained. Next, we have applied our model to treat a disordered ferromagnetic bulk compound in the free electron approximation, weak-disorder and the weak-relativistic limits. By this means, we have obtained explicit expressions of the anomalous Hall conductivity for both skew-scattering and side-jump contributions. In addition, we have highlighted the difference concerning the Feynmann diagrams describing the side-jump mechanism in the Dirac and Pauli approaches and have shown that it corresponds to different vertex renormalizations.

equal to $1/k_B T$, ρ_0 is the density matrix in equilibrium in absence of perturbation, J_i is the i-component of the current density operator in the Heisenberg representation and $\langle \dots \rangle_c$ denotes the average over all the disordered configurations. In the independent electrons approximation, we have

$$\langle n | J_i(t + i\hbar\lambda) | m \rangle = e^{\frac{i\hbar}{\hbar}(t + i\hbar\lambda)(\varepsilon_n - \varepsilon_m)} \langle n | \tilde{J}_i | m \rangle, \quad (A2)$$

where we have used $H = \sum_n \varepsilon_n a_n^\dagger a_n$ and defined \tilde{J} as the current density operator in the Schrödinger representation. Using the relation $\text{Tr}[\rho_0 a_m^\dagger a_n a_p^\dagger a_q] = \delta_{mq} \delta_{np} f(\varepsilon_m)(1 - f(\varepsilon_n))$ where $f(\varepsilon)$ is the Fermi-Dirac distribution function, we get

$$\tilde{\sigma}_{ij}(\omega) = \Omega \lim_{s \rightarrow 0^+} \int_0^\beta d\lambda e^{-\lambda(\varepsilon_n - \varepsilon_m)} \int_0^{+\infty} dt \sum_{nm} \left\langle f(\varepsilon_m)(1 - f(\varepsilon_n)) e^{\frac{i\hbar}{\hbar}(-\hbar\omega + is + \varepsilon_n - \varepsilon_m)} \langle m | \tilde{J}_j | n \rangle \langle n | \tilde{J}_i | m \rangle \right\rangle_c. \quad (A3)$$

The integration over λ leads to a factor $(1 - e^{-\beta(\varepsilon_n - \varepsilon_m)})/(\varepsilon_n - \varepsilon_m)$ which can be simplified with $f(\varepsilon_m)(1 - f(\varepsilon_n))$ as

$$\frac{1 - e^{-\beta(\varepsilon_n - \varepsilon_m)}}{\varepsilon_n - \varepsilon_m} f(\varepsilon_m)(1 - f(\varepsilon_n)) = \frac{f(\varepsilon_m) - f(\varepsilon_n)}{\varepsilon_n - \varepsilon_m}, \quad (\text{A4})$$

reporting this in (A3), we obtain

$$\tilde{\sigma}_{ij}(\omega) = \Omega \lim_{s \rightarrow 0^+} \int_0^{+\infty} dt \sum_{nm} \left\langle e^{\frac{it}{\hbar}(-\hbar\omega + is + \varepsilon_n - \varepsilon_m)} \frac{f(\varepsilon_m) - f(\varepsilon_n)}{\varepsilon_n - \varepsilon_m} \langle m | \tilde{J}_j | n \rangle \langle n | \tilde{J}_i | m \rangle \right\rangle_c. \quad (\text{A5})$$

The integration over t gives

$$\tilde{\sigma}_{ij}(\omega) = i\hbar \Omega \lim_{s \rightarrow 0^+} \sum_{nm} \left\langle \frac{f(\varepsilon_m) - f(\varepsilon_n)}{(\varepsilon_n - \varepsilon_m)(\varepsilon_n - \varepsilon_m - \hbar\omega + is)} \langle m | \tilde{J}_j | n \rangle \langle n | \tilde{J}_i | m \rangle \right\rangle_c. \quad (\text{A6})$$

We shall now make some transformations of this expression in order to get the Bastin formula.

We restrict our derivation to zero frequency (from now, we drop the ω variable). After introducing the identity $\int_{-\infty}^{+\infty} d\varepsilon \delta(\varepsilon - H) = 1$ in (A6), we obtain

$$\begin{aligned} \tilde{\sigma}_{ij} = i\hbar \Omega \lim_{s \rightarrow 0^+} \int_{-\infty}^{+\infty} d\varepsilon \sum_{nm} \left\langle \left(\frac{f(\varepsilon)\delta(\varepsilon - \varepsilon_m)}{(\varepsilon_n - \varepsilon)(\varepsilon_n - \varepsilon + is)} \right. \right. \\ \left. \left. - \frac{f(\varepsilon)\delta(\varepsilon - \varepsilon_n)}{(\varepsilon - \varepsilon_m)(\varepsilon - \varepsilon_m + is)} \right) \langle m | \tilde{J}_j | n \rangle \langle n | \tilde{J}_i | m \rangle \right\rangle_c. \quad (\text{A7}) \end{aligned}$$

We remark that

$$\lim_{s \rightarrow 0^+} \frac{1}{(\varepsilon_n - \varepsilon)(\varepsilon_n - \varepsilon + is)} = \lim_{s \rightarrow 0^+} \frac{d}{d\varepsilon} \left(\frac{1}{\varepsilon_n - \varepsilon + is} \right); \quad (\text{A8})$$

then we have

$$\begin{aligned} \tilde{\sigma}_{ij} = -i\hbar \Omega \lim_{s \rightarrow 0^+} \int_{-\infty}^{+\infty} d\varepsilon f(\varepsilon) \\ \times \sum_{nm} \left\langle \langle m | \tilde{J}_j | n \rangle \frac{d}{d\varepsilon} \left(\frac{1}{\varepsilon - \varepsilon_n - is} \right) \langle n | \tilde{J}_i | m \rangle \delta(\varepsilon - \varepsilon_m) \right. \\ \left. - \langle m | \tilde{J}_j | n \rangle \delta(\varepsilon - \varepsilon_n) \langle n | \tilde{J}_i | m \rangle \frac{d}{d\varepsilon} \left(\frac{1}{\varepsilon - \varepsilon_m + is} \right) \right\rangle_c, \quad (\text{A9}) \end{aligned}$$

which can be expressed as

$$\begin{aligned} \tilde{\sigma}_{ij} = \frac{ie^2\hbar}{\Omega} \int_{-\infty}^{+\infty} d\varepsilon f(\varepsilon) \text{Tr} \left\langle v_i \frac{dG^+(\varepsilon)}{d\varepsilon} v_j \delta(\varepsilon - H) \right. \\ \left. - v_i \delta(\varepsilon - H) v_j \frac{dG^-(\varepsilon)}{d\varepsilon} \right\rangle_c, \quad (\text{A10}) \end{aligned}$$

where we have introduced the Green's function $G^\pm(\varepsilon) = \lim_{s \rightarrow 0^+} (\varepsilon - H \pm is)^{-1}$ and the velocity through the relation $\tilde{\mathbf{J}} = -e\mathbf{v}/\Omega$. This expression for the conductivity was first obtained by Bastin *et al.*³¹ but in the particular case of a Schrödinger Hamiltonian and made explicit use of the form taken by the velocity operator in the Schrödinger case. The present derivation is more general in the sense that it is independent of the explicit form of the velocity operator and is therefore valid both for the Schrödinger, Pauli and Dirac cases. The only restriction is the independent electrons approximation. This formula, called Bastin formula, is interesting because it expresses the conductivity as a product of velocities and Green's functions. However, it is still difficult to calculate because of the integration over the energy ε . By making an integration by parts, a factor $df(\varepsilon)/d\varepsilon$ appears instead of the factor $f(\varepsilon)$ and the integration interval will be thus reduced.

In (A10), we express the delta function in terms of Green's functions using $\delta(\varepsilon - H) = -(G^+(\varepsilon) - G^-(\varepsilon))/2i\pi$. We keep one half of this expression and make an integration by parts on the second half, then we get

$$\begin{aligned} \tilde{\sigma}_{ij} = -\frac{e^2\hbar}{4\pi\Omega} \int_{-\infty}^{+\infty} d\varepsilon \frac{df(\varepsilon)}{d\varepsilon} \text{Tr} \left\langle v_i (G^+(\varepsilon) - G^-(\varepsilon)) v_j G^-(\varepsilon) - v_i G^+(\varepsilon) v_j (G^+(\varepsilon) - G^-(\varepsilon)) \right\rangle_c \\ + \frac{e^2\hbar}{4\pi\Omega} \int_{-\infty}^{+\infty} d\varepsilon f(\varepsilon) \text{Tr} \left\langle v_i \frac{dG^-(\varepsilon)}{d\varepsilon} v_j G^-(\varepsilon) - v_i G^-(\varepsilon) v_j \frac{dG^-(\varepsilon)}{d\varepsilon} + v_i G^+(\varepsilon) v_j \frac{dG^+(\varepsilon)}{d\varepsilon} - v_i \frac{dG^+(\varepsilon)}{d\varepsilon} v_j G^+(\varepsilon) \right\rangle_c, \quad (\text{A11}) \end{aligned}$$

the second term in this expression can be simplified by using the relations $dG^\pm(\varepsilon)/d\varepsilon = -(G^\pm(\varepsilon))^2$ and $i\hbar v_i = [r_i, H] = -[r_i, G^{-1}]$ and by performing once more an integration by parts. Finally, the conductivity can be written as a sum of two terms: $\tilde{\sigma}_{ij} = \tilde{\sigma}_{ij}^I + \tilde{\sigma}_{ij}^{II}$ where

$$\begin{aligned} \tilde{\sigma}_{ij}^I = & -\frac{e^2\hbar}{4\pi\Omega} \int_{-\infty}^{+\infty} d\varepsilon \frac{df(\varepsilon)}{d\varepsilon} \\ & \times \text{Tr} \left\langle v_i (G^+(\varepsilon) - G^-(\varepsilon)) v_j G^-(\varepsilon) \right. \\ & \left. - v_i G^+(\varepsilon) v_j (G^+(\varepsilon) - G^-(\varepsilon)) \right\rangle_c, \end{aligned} \quad (\text{A12})$$

and

$$\begin{aligned} \tilde{\sigma}_{ij}^{II} = & \frac{e^2}{4i\pi\Omega} \int_{-\infty}^{+\infty} d\varepsilon \frac{df(\varepsilon)}{d\varepsilon} \\ & \times \text{Tr} \left\langle (G^+(\varepsilon) - G^-(\varepsilon)) (r_i v_j - r_j v_i) \right\rangle_c. \end{aligned} \quad (\text{A13})$$

(A12) and (A13) correspond to the formula obtained by Streda³² in the Schrödinger case. The present derivation shows that it holds also in the Pauli and Dirac cases. For the diagonal components of the conductivity tensor, $\tilde{\sigma}_{ij}^{II}$ is equal to zero and we obtain the Kubo-Greenwood formula²⁹

$$\begin{aligned} \tilde{\sigma}_{ii} = & \frac{e^2\hbar}{4\pi\Omega} \int_{-\infty}^{+\infty} d\varepsilon \frac{df(\varepsilon)}{d\varepsilon} \text{Tr} \left\langle v_i (G^+(\varepsilon) - G^-(\varepsilon)) \right. \\ & \left. \times v_i (G^+(\varepsilon) - G^-(\varepsilon)) \right\rangle_c. \end{aligned} \quad (\text{A14})$$

At zero temperature, the factor $df(\varepsilon)/d\varepsilon$ is equal to $-\delta(\varepsilon - \varepsilon_F)$, only electrons at the Fermi level contribute to the conductivity (for both diagonal and off-diagonal

components). In conclusion, at $\omega = 0$ and $T = 0$, the conductivity tensor can be expressed as a sum of two terms $\tilde{\sigma}_{ij} = \tilde{\sigma}_{ij}^I + \tilde{\sigma}_{ij}^{II}$ with

$$\begin{aligned} \tilde{\sigma}_{ij}^I = & \frac{e^2\hbar}{4\pi\Omega} \text{Tr} \left\langle v_i (G^+ - G^-) v_j G^- \right. \\ & \left. - v_i G^+ v_j (G^+ - G^-) \right\rangle_c, \end{aligned} \quad (\text{A15})$$

and,

$$\tilde{\sigma}_{ij}^{II} = -\frac{e^2}{4i\pi\Omega} \text{Tr} \left\langle (G^+ - G^-) (r_i v_j - r_j v_i) \right\rangle_c, \quad (\text{A16})$$

where we have dropped the energy reference ε_F by introducing the Green's functions at the Fermi level $G^\pm = G(\varepsilon_F \pm i0) = (\varepsilon_F \pm i0 - H)^{-1}$.

APPENDIX B: STREDA FORMULA IN THE WEAK-RELATIVISTIC LIMIT

In this appendix, we give the detail of the calculation concerning the weak-relativistic expansion of the Streda conductivity starting from the Dirac equation. From (A15), we see that $\tilde{\sigma}_{ij}^I$ is a combination of terms like

$$\Lambda_{ij}(z_1, z_2) = \frac{e^2\hbar}{4\pi\Omega} \text{Tr} \left\langle v_i G(z_1) v_j G(z_2) \right\rangle_c, \quad (\text{B1})$$

where z_1 and z_2 are equals to $(\varepsilon_F \pm i0)$. When we report the Dirac velocity (17) and the Dirac Green's function (19) in (B1), make the explicit product of the 4 operators and take the trace over the lower and upper components of the wave function, we obtain the general form:

$$\begin{aligned} \Lambda_{ij}(z_1, z_2) = & \frac{e^2\hbar}{4\pi\Omega} \text{Tr} \left\langle \sigma_i D(z_1) \frac{\boldsymbol{\sigma} \cdot \mathbf{p}}{2m} \tilde{G}(z_1) \sigma_j D(z_2) \frac{\boldsymbol{\sigma} \cdot \mathbf{p}}{2m} \tilde{G}(z_2) \right. \\ & + \sigma_i \tilde{G}(z_1) \frac{\boldsymbol{\sigma} \cdot \mathbf{p}}{2m} Q^{-1}(z_1) D(z_1) Q(z_1) \sigma_j \tilde{G}(z_2) \frac{\boldsymbol{\sigma} \cdot \mathbf{p}}{2m} Q^{-1}(z_2) D(z_2) Q(z_2) \\ & + \sigma_i D(z_1) \left(\frac{1}{2m} + \frac{\boldsymbol{\sigma} \cdot \mathbf{p}}{2m} \tilde{G}(z_1) \frac{\boldsymbol{\sigma} \cdot \mathbf{p}}{2m} \right) \sigma_j \left(\tilde{G}(z_2) - \tilde{G}(z_2) \frac{\boldsymbol{\sigma} \cdot \mathbf{p}}{2mc} (z_2 - V - \mu_B(\boldsymbol{\sigma} \cdot \mathbf{B} \text{eff})) D(z_2) \frac{\boldsymbol{\sigma} \cdot \mathbf{p}}{2mc} \tilde{G}(z_2) \right) \\ & \left. + \sigma_i \left(\tilde{G}(z_1) - \tilde{G}(z_1) \frac{\boldsymbol{\sigma} \cdot \mathbf{p}}{2mc} (z_1 - V - \mu_B(\boldsymbol{\sigma} \cdot \mathbf{B} \text{eff})) D(z_1) \frac{\boldsymbol{\sigma} \cdot \mathbf{p}}{2mc} \tilde{G}(z_1) \right) \sigma_j D(z_2) \left(\frac{1}{2m} + \frac{\boldsymbol{\sigma} \cdot \mathbf{p}}{2m} \tilde{G}(z_2) \frac{\boldsymbol{\sigma} \cdot \mathbf{p}}{2m} \right) \right\rangle_c. \end{aligned} \quad (\text{B2})$$

Similarly, when we report (17) and (19) in (A16), we get

$$\tilde{\sigma}_{ij}^{II} = -\frac{e^2}{4i\pi\Omega} \text{Tr} \left\langle \left(\tilde{G}^+ \frac{\boldsymbol{\sigma} \cdot \mathbf{p}}{2m} Q^+ D^+ Q^+ + D^+ \frac{\boldsymbol{\sigma} \cdot \mathbf{p}}{2m} \tilde{G}^+ - \tilde{G}^- \frac{\boldsymbol{\sigma} \cdot \mathbf{p}}{2m} Q^- D^- Q^- - D^- \frac{\boldsymbol{\sigma} \cdot \mathbf{p}}{2m} \tilde{G}^- \right) (r_i \sigma_j - r_j \sigma_i) \right\rangle_c. \quad (\text{B3})$$

Expressions (B2) and (B3) are exact expressions without any assumption on the value of c . We will now calculate the weak-relativistic expansion of these expressions at orders $1/c^0$ and $1/c^2$ in order to compare them with the expression obtained from the Pauli approach.

1. Dirac conductivity at order $1/c^0$

In the non-relativistic limit, D is simply equal to the unit matrix 1 (see (20)), thus (B2) reduces to

$$\Lambda_{ij}^{(0)}(z_1, z_2) = \frac{e^2 \hbar}{4\pi\Omega} \text{Tr} \left\langle \sigma_i \frac{\boldsymbol{\sigma} \cdot \mathbf{p}}{2m} \tilde{G}(z_1) \sigma_j \frac{\boldsymbol{\sigma} \cdot \mathbf{p}}{2m} \tilde{G}(z_2) + \sigma_i \tilde{G}(z_1) \frac{\boldsymbol{\sigma} \cdot \mathbf{p}}{2m} \sigma_j \tilde{G}(z_2) \frac{\boldsymbol{\sigma} \cdot \mathbf{p}}{2m} \right. \\ \left. + \sigma_i \left(\frac{1}{2m} + \frac{\boldsymbol{\sigma} \cdot \mathbf{p}}{2m} \tilde{G}(z_1) \frac{\boldsymbol{\sigma} \cdot \mathbf{p}}{2m} \right) \sigma_j \tilde{G}(z_2) + \sigma_i \tilde{G}(z_1) \sigma_j \left(\frac{1}{2m} + \frac{\boldsymbol{\sigma} \cdot \mathbf{p}}{2m} \tilde{G}(z_2) \frac{\boldsymbol{\sigma} \cdot \mathbf{p}}{2m} \right) \right\rangle_c, \quad (\text{B4})$$

which can be rewritten as

$$\Lambda_{ij}^{(0)}(z_1, z_2) = \frac{e^2 \hbar}{4\pi\Omega} \text{Tr} \left\langle \frac{p_i}{m} \tilde{G}(z_1) \frac{p_j}{m} \tilde{G}(z_2) \right. \\ \left. + \frac{1}{2m} \left(\sigma_i \sigma_j \tilde{G}(z_2) + \sigma_j \sigma_i \tilde{G}(z_1) \right) \right\rangle_c, \quad (\text{B5})$$

where we have used the fact that $\sigma_i (\boldsymbol{\sigma} \cdot \mathbf{p}) + (\boldsymbol{\sigma} \cdot \mathbf{p}) \sigma_i = 2p_i$. When we report this expression in (A15), the conductivity $\tilde{\sigma}_{ij}^I$ at order $1/c^0$ is

$$\tilde{\sigma}_{ij}^{I(0)} = \frac{e^2 \hbar}{4\pi\Omega} \text{Tr} \left\langle \frac{p_i}{m} (\tilde{G}^+ - \tilde{G}^-) \frac{p_j}{m} \tilde{G}^- \right. \\ \left. - \frac{p_i}{m} \tilde{G}^+ + \frac{p_j}{m} (\tilde{G}^+ - \tilde{G}^-) \right\rangle_c \\ + \varepsilon_{ijk} \frac{e^2 \hbar}{4i\pi m \Omega} \text{Tr} \left\langle \sigma_k (\tilde{G}^+ - \tilde{G}^-) \right\rangle_c, \quad (\text{B6})$$

where $\varepsilon_{ijk} = 1$ if $\{i, j, k\} = \{x, y, z\}$ or cyclic permutations and $\varepsilon_{ijk} = 0$ otherwise. This factor is introduced through the term $(\sigma_i \sigma_j - \sigma_j \sigma_i) = 2i\varepsilon_{ijk} \sigma_k$. The first term in the right hand side corresponds exactly to the contribution that we get in a non-relativistic description because in this case the velocity is $\tilde{\mathbf{v}} = \mathbf{p}/m$ and the Green's function is simply the non-relativistic Green's function \tilde{G} . On the contrary, the second term is not present in the Pauli approach and should not appear when we take the non-relativistic limit in the Dirac approach. In fact, we show that this term is exactly cancelled by a term in $\tilde{\sigma}_{ij}^{II(0)}$. Replacing D by 1 in (B3), we get $\tilde{\sigma}_{ij}^{II}$ at order $1/c^0$

$$\tilde{\sigma}_{ij}^{II(0)} = -\frac{e^2}{8i\pi m \Omega} \text{Tr} \left\langle (\tilde{G}^+ - \tilde{G}^-) ((\boldsymbol{\sigma} \cdot \mathbf{p}) (r_i \sigma_j - r_j \sigma_i)) \right\rangle_c$$

$$+ (r_i \sigma_j - r_j \sigma_i) (\boldsymbol{\sigma} \cdot \mathbf{p})) \rangle_c. \quad (\text{B7})$$

The relations $(\boldsymbol{\sigma} \cdot \mathbf{A})(\boldsymbol{\sigma} \cdot \mathbf{B}) = (\mathbf{A} \cdot \mathbf{B}) + i\boldsymbol{\sigma} \cdot (\mathbf{A} \times \mathbf{B})$ and $[r_i, p_j] = i\hbar\delta_{ij}$, allow to rewrite (B7) as

$$\tilde{\sigma}_{ij}^{II(0)} = -\frac{e^2}{4i\pi\Omega} \text{Tr} \left\langle (\tilde{G}^+ - \tilde{G}^-) \left(r_i \frac{p_j}{m} - r_j \frac{p_i}{m} \right) \right\rangle_c \\ - \varepsilon_{ijk} \frac{e^2 \hbar}{4i\pi m \Omega} \text{Tr} \left\langle \sigma_k (\tilde{G}^+ - \tilde{G}^-) \right\rangle_c. \quad (\text{B8})$$

The second term in the right hand side cancels the supplementary term in (B6) and we obtain finally for the total conductivity at order $1/c^0$

$$\tilde{\sigma}_{ij}^{(0)} = \tilde{\sigma}_{ij}^{I(0)} + \tilde{\sigma}_{ij}^{II(0)} \\ = \frac{e^2 \hbar}{4\pi\Omega} \text{Tr} \left\langle \frac{p_i}{m} (\tilde{G}^+ - \tilde{G}^-) \frac{p_j}{m} \tilde{G}^- - \frac{p_i}{m} \tilde{G}^+ + \frac{p_j}{m} (\tilde{G}^+ - \tilde{G}^-) \right\rangle_c \\ - \frac{e^2}{4i\pi\Omega} \text{Tr} \left\langle (\tilde{G}^+ - \tilde{G}^-) \left(r_i \frac{p_j}{m} - r_j \frac{p_i}{m} \right) \right\rangle_c, \quad (\text{B9})$$

which corresponds exactly to the total conductivity obtained from (A15) and (A16) when we report the non-relativistic Pauli velocity $\tilde{\mathbf{v}} = \mathbf{p}/m$ and the non-relativistic Pauli Green's function \tilde{G} .

2. Dirac conductivity at order $1/c^2$

To get $\tilde{\sigma}_{ij}$ at order $1/c^2$, it is necessary to take into account the next terms in the expansion of D : $D(z) \approx 1 - Q(z)(z - V - \mu_B(\boldsymbol{\sigma} \cdot \mathbf{B}_{eff}))/2mc^2$. Thus, from (B2), we get

$$\Lambda_{ij}^{(2)}(z_1, z_2) = \frac{e^2 \hbar}{4\pi\Omega} \text{Tr} \left\langle \frac{p_i}{m} \tilde{G}(z_1) (\mathbf{v}_{rc})_j \tilde{G}(z_2) + (\mathbf{v}_{rc})_j \tilde{G}(z_1) \frac{p_j}{m} \tilde{G}(z_2) \right. \\ \left. + \frac{p_i}{m} \tilde{G}(z_1) \frac{p_j}{m} \tilde{G}(z_2) H_{rc} \tilde{G}(z_2) + \frac{p_i}{m} \tilde{G}(z_1) H_{rc} \tilde{G}(z_1) \frac{p_j}{m} \tilde{G}(z_2) \right. \\ \left. - \frac{1}{8m^3 c^2} \left(\sigma_i \sigma_j \tilde{G}(z_2) \boldsymbol{\sigma} \cdot \mathbf{p} (z_2 - V - \mu_B(\boldsymbol{\sigma} \cdot \mathbf{B}_{eff})) \boldsymbol{\sigma} \cdot \mathbf{p} \tilde{G}(z_2) + \sigma_j \sigma_i \tilde{G}(z_1) \boldsymbol{\sigma} \cdot \mathbf{p} (z_1 - V - \mu_B(\boldsymbol{\sigma} \cdot \mathbf{B}_{eff})) \boldsymbol{\sigma} \cdot \mathbf{p} \tilde{G}(z_1) \right) \right\rangle_c$$

$$\begin{aligned}
& -\frac{1}{2m^3c^2}p_i p_j \left(\tilde{G}(z_1) + \tilde{G}(z_2) \right) - \frac{1}{4m^2c^2} \left(\sigma_i(z_1 - V - \mu_B(\boldsymbol{\sigma} \cdot \mathbf{B}_{eff}))\sigma_j \tilde{G}(z_2) + \sigma_j(z_2 - V - \mu_B(\boldsymbol{\sigma} \cdot \mathbf{B}_{eff}))\sigma_i \tilde{G}(z_1) \right) \\
& - \frac{i}{4m^3c^2}(z_1 - z_2) \left((\mathbf{p} \times \boldsymbol{\sigma})_i \tilde{G}(z_1) p_j \tilde{G}(z_2) - p_i \tilde{G}(z_1) (\mathbf{p} \times \boldsymbol{\sigma})_j \tilde{G}(z_2) \right) \Bigg\rangle_c, \tag{B10}
\end{aligned}$$

where H_{rc} and \mathbf{v}_{rc} are the relativistic corrections at order $1/c^2$ to the Hamiltonian and the velocity respectively given by (13) and (14). The last term in the right side hand does not contribute because $(z_1 - z_2) \rightarrow 0$. Reporting the expression (B10) in the conductivity (A15), we get $\tilde{\sigma}_{ij}^I$ at order $1/c^2$

$$\begin{aligned}
\tilde{\sigma}_{ij}^{I(2)} &= \frac{e^2 \hbar}{4\pi\Omega} \text{Tr} \left\langle (\mathbf{v}_{rc})_i (\tilde{G}^+ - \tilde{G}^-) \frac{p_j}{m} \tilde{G}^- - (\mathbf{v}_{rc})_i \tilde{G}^+ \frac{p_j}{m} (\tilde{G}^+ - \tilde{G}^-) + \frac{p_i}{m} (\tilde{G}^+ - \tilde{G}^-) (\mathbf{v}_{rc})_j \tilde{G}^- \right. \\
& - \frac{p_i}{m} \tilde{G}^+ (\mathbf{v}_{rc})_j (\tilde{G}^+ - \tilde{G}^-) + \frac{p_i}{m} (\tilde{G}^+ H_{rc} \tilde{G}^+ - \tilde{G}^- H_{rc} \tilde{G}^-) \frac{p_j}{m} \tilde{G}^- + \frac{p_i}{m} (\tilde{G}^+ - \tilde{G}^-) \frac{p_j}{m} \tilde{G}^- H_{rc} \tilde{G}^- \\
& \left. - \frac{p_i}{m} \tilde{G}^+ H_{rc} \tilde{G}^+ + \frac{p_j}{m} (\tilde{G}^+ - \tilde{G}^-) - \frac{p_i}{m} \tilde{G}^+ + \frac{p_j}{m} (\tilde{G}^+ H_{rc} \tilde{G}^+ - \tilde{G}^- H_{rc} \tilde{G}^-) \right\rangle_c \\
& - \varepsilon_{ijk} \frac{e^2 \hbar}{16i\pi m^3 c^2 \Omega} \text{Tr} \left\langle \left(\tilde{G}^+ \boldsymbol{\sigma} \cdot \mathbf{p} (\varepsilon_F - V - \mu_B(\boldsymbol{\sigma} \cdot \mathbf{B}_{eff})) \boldsymbol{\sigma} \cdot \mathbf{p} \tilde{G}^+ - \tilde{G}^- \boldsymbol{\sigma} \cdot \mathbf{p} (\varepsilon_F - V - \mu_B(\boldsymbol{\sigma} \cdot \mathbf{B}_{eff})) \boldsymbol{\sigma} \cdot \mathbf{p} \tilde{G}^- \right) \sigma_k \right\rangle_c \\
& + \frac{e^2 \hbar}{16\pi m^2 c^2 \Omega} \text{Tr} \left\langle (\tilde{G}^+ - \tilde{G}^-) (\sigma_i (\varepsilon_F - V - \mu_B(\boldsymbol{\sigma} \cdot \mathbf{B}_{eff})) \sigma_j - \sigma_j (\varepsilon_F - V - \mu_B(\boldsymbol{\sigma} \cdot \mathbf{B}_{eff})) \sigma_i) \right\rangle_c. \tag{B11}
\end{aligned}$$

The first term corresponds exactly to the relativistic corrections that we get at order $1/c^2$ in the Pauli approach. The two last terms are supplementary terms which should not appear. We show that they are cancelled by terms in $\tilde{\sigma}_{ij}^{II(2)}$. Indeed, when we expand D up to the second order in $1/c$ in the expression (B3) of $\tilde{\sigma}_{ij}^{II}$, we obtain

$$\begin{aligned}
\tilde{\sigma}_{ij}^{II(2)} &= -\frac{e^2}{4i\pi\Omega} \text{Tr} \left\langle \left(\tilde{G}^+ H_{rc} \tilde{G}^+ - \tilde{G}^- H_{rc} \tilde{G}^- \right) \left(r_i \frac{p_j}{m} - r_j \frac{p_i}{m} \right) + \left(\tilde{G}^+ - \tilde{G}^- \right) (r_i (\mathbf{v}_{rc})_j - r_j (\mathbf{v}_{rc})_i) \right\rangle_c \\
& + \varepsilon_{ijk} \frac{e^2 \hbar}{16i\pi m^3 c^2 \Omega} \text{Tr} \left\langle \left(\tilde{G}^+ \boldsymbol{\sigma} \cdot \mathbf{p} (\varepsilon_F - V - \mu_B(\boldsymbol{\sigma} \cdot \mathbf{B}_{eff})) \boldsymbol{\sigma} \cdot \mathbf{p} \tilde{G}^+ - \tilde{G}^- \boldsymbol{\sigma} \cdot \mathbf{p} (\varepsilon_F - V - \mu_B(\boldsymbol{\sigma} \cdot \mathbf{B}_{eff})) \boldsymbol{\sigma} \cdot \mathbf{p} \tilde{G}^- \right) \sigma_k \right\rangle_c \\
& - \frac{e^2 \hbar}{16\pi m^2 c^2 \Omega} \text{Tr} \left\langle (\tilde{G}^+ - \tilde{G}^-) (\sigma_i (\varepsilon_F - V - \mu_B(\boldsymbol{\sigma} \cdot \mathbf{B}_{eff})) \sigma_j - \sigma_j (\varepsilon_F - V - \mu_B(\boldsymbol{\sigma} \cdot \mathbf{B}_{eff})) \sigma_i) \right\rangle_c. \tag{B12}
\end{aligned}$$

The two last terms in the right hand side cancel the supplementary terms in (B11) and we obtain finally for the total conductivity at order $1/c^2$

$$\begin{aligned}
\tilde{\sigma}_{ij}^{(2)} &= \tilde{\sigma}_{ij}^{I(2)} + \tilde{\sigma}_{ij}^{II(2)} = \frac{e^2 \hbar}{4\pi\Omega} \text{Tr} \left\langle (\mathbf{v}_{rc})_i (\tilde{G}^+ - \tilde{G}^-) \frac{p_j}{m} \tilde{G}^- - (\mathbf{v}_{rc})_i \tilde{G}^+ \frac{p_j}{m} (\tilde{G}^+ - \tilde{G}^-) \right. \\
& + \frac{p_i}{m} (\tilde{G}^+ - \tilde{G}^-) (\mathbf{v}_{rc})_j \tilde{G}^- - \frac{p_i}{m} \tilde{G}^+ (\mathbf{v}_{rc})_j (\tilde{G}^+ - \tilde{G}^-) + \frac{p_i}{m} (\tilde{G}^+ H_{rc} \tilde{G}^+ - \tilde{G}^- H_{rc} \tilde{G}^-) \frac{p_j}{m} \tilde{G}^- \\
& + \frac{p_i}{m} (\tilde{G}^+ - \tilde{G}^-) \frac{p_j}{m} \tilde{G}^- H_{rc} \tilde{G}^- - \frac{p_i}{m} \tilde{G}^+ H_{rc} \tilde{G}^+ + \frac{p_j}{m} (\tilde{G}^+ - \tilde{G}^-) - \frac{p_i}{m} \tilde{G}^+ + \frac{p_j}{m} (\tilde{G}^+ H_{rc} \tilde{G}^+ - \tilde{G}^- H_{rc} \tilde{G}^-) \Bigg\rangle_c \\
& - \frac{e^2}{4i\pi\Omega} \text{Tr} \left\langle \left(\tilde{G}^+ H_{rc} \tilde{G}^+ - \tilde{G}^- H_{rc} \tilde{G}^- \right) \left(r_i \frac{p_j}{m} - r_j \frac{p_i}{m} \right) + \left(\tilde{G}^+ - \tilde{G}^- \right) (r_i (\mathbf{v}_{rc})_j - r_j (\mathbf{v}_{rc})_i) \right\rangle_c. \tag{B13}
\end{aligned}$$

This expression corresponds exactly to the one that we get in the Pauli approach when we report the Pauli velocity at order $1/c^2$, \mathbf{v}_{rc} , and the Pauli Hamiltonian at order $1/c^2$, H_{rc} , in (A15) and (A16). For higher order terms (say of order $1/c^{2n}$ with $n > 1$), we can predict that similar cancellations occur when we consider the total conductivity $\tilde{\sigma}_{ij}^{I(2n)} + \tilde{\sigma}_{ij}^{II(2n)}$. We have thus proved in this appendix the consistence between the Pauli conductivity and the weak-relativistic limit of the Dirac

conductivity.

* Electronic address: crepieux@mpi-halle.mpg.de

- ¹ F.P. Beitel and E.M. Pugh, Phys. Rev. **112**, 1516 (1958).
- ² H. Ashworth, D. Sengupta, G. Schnakenberg, L. Shapiro, and L. Berger, Phys. Rev. **185**, 792 (1969).
- ³ A.K. Majumdar and L. Berger, Phys. Rev. B **7**, 4203 (1973).
- ⁴ R.C. O'Handley, Phys. Rev. B **18**, 2577 (1978).
- ⁵ A. Sinha and A.K. Majumdar, J. Appl. Phys. **50**, 7533 (1979).
- ⁶ A.B. Pakhomov, X. Yan, N. Wang, X.N. Jing, B. Zhao, K.K. Fng, J. Xhie, T.F. Hng, S.K. Wong, Physica A **241**, 344 (1997); J.C. Denardin, A.B. Pakhomov, M. Knobel, H. Liu, and X.X. Zhang, J. Phys.: Condens. Matter **12**, 3397 (2000).
- ⁷ J. Caulet, C. Train, V. Mathet, R. Laval, B. Bartenlian, P. Veillet, K. Le Dang, and C. Chappert, JMMM **198**, 318 (1999).
- ⁸ H. Sato, T. Kumano, Y. Aoki, T. Kaneko, and R. Yamamoto, J. Phys. Soc. Jpn. **62**, 416 (1993); C.L. Canedy, X.W. Li and G. Xiao, J. Appl. Phys. **81**, 5367 (1997).
- ⁹ H. Ohno, D. Chiba, F. Matsukura, T. Omiya, E. Abe, T. Dietl, Y. Ohno, and K. Ohtani, Nature **408**, 944 (2000).
- ¹⁰ J. Wunderlich, D. Ravelosona, C. Chappert, V. Mathet, J. Ferré, and J.-P. Jamet, private communication.
- ¹¹ S. de Haan and J.C. Lodder, JMMM **168**, 321 (1997); S. Nagagawa, K. Takayama, A. Sato, and M. Naoe, J. Appl. Phys. **85**, 4592 (1999).
- ¹² R. Karplus and J.M. Luttinger, Phys. Rev. **95**, 1154 (1954).
- ¹³ J. Smit, Physica **21**, 877 (1955); J. Smit, Physica **24**, 39 (1958).
- ¹⁴ J.M. Luttinger, Phys. Rev. **112**, 739 (1958).
- ¹⁵ L. Berger, Phys. Rev. B **2**, 4559 (1970); L. Berger, Phys. Rev. B **5**, 1862 (1972).
- ¹⁶ J. Smit, Phys. Rev. B **8**, 2349 (1973); L. Berger, Phys. Rev. B **8**, 2351 (1973).
- ¹⁷ S.K. Lyo and T. Holstein, Phys. Rev. B **9**, 2412 (1974).
- ¹⁸ J. Smit, Phys. Rev. B **17**, 1450 (1978); L. Berger, Phys. Rev. B **17**, 1453 (1978).
- ¹⁹ P. Nozières and C. Lewiner, J. de Phys. **34**, 901 (1973).
- ²⁰ C. Lewiner, O. Betbeder-Matibet and P. Nozières, J. Phys. Chem. Solids **34**, 765 (1973).
- ²¹ S.K. Lyo and T. Holstein, Phys. Rev. Lett. **29**, 423 (1972).
- ²² *The Hall effect and its applications*, edited by C.L. Chien and C.R. Westgate (Plenum Press, New-York and London, 1980).
- ²³ YE. I. Kondorskii, A.V. Vedyayev, and A.B. Granovskii, Fiz. Metal. Metallov. **40**, 455 (1975); YE. I. Kondorskii, A.V. Vedyayev, and A.B. Granovskii, Fiz. Metal. Metallov. **40**, 903 (1975).
- ²⁴ A.H. MacDonald and S.H. Vosko, J. Phys. C: Solid State Phys. **12**, 2977 (1979).
- ²⁵ Eq. (16) is actually an approximate form of the Kohn-Sham-Dirac equation, $H = c\boldsymbol{\alpha} \cdot (\mathbf{p} - e\mathbf{A}) + \beta mc^2 + V$, generally used to treat relativistic effects in magnetic system. The calculations presented in Sec. III and Appendix B have also been performed starting from the Kohn-Sham-Dirac equation, in particular the check of the Dirac conductivity in the weak-relativistic limit which presents the same characteristic, namely a cancellation of the supplementary terms when one consider the total conductivity $\bar{\sigma}^I + \bar{\sigma}^{II}$.
- ²⁶ W.H. Butler, Phys. Rev. B **31**, 3260 (1985).
- ²⁷ J. Banhart and H. Ebert, Europhys. Lett. **32**, 517 (1995); J. Banhart, A. Vernes, and H. Ebert, Solid State Commun. **98**, 129 (1996).
- ²⁸ P. Weinberger, P.M. Levy, J. Banhard, L. Szunyogh, and B. Ujfalussy, J. Phys.: Condens. Matter **8**, 7677 (1996).
- ²⁹ D.A. Greenwood, Proc. Phys. Soc. **71**, 585 (1958).
- ³⁰ R. Kubo, Canad. J. Phys. **34**, 1274 (1956); R. Kubo, J. Phys. Soc. Japan **12**, 570 (1957).
- ³¹ A. Bastin, C. Lewiner, O. Betbeder-Matibet, and P. Nozières, J. Phys. Chem. Solids **32**, 1811 (1971).
- ³² P. Štředa, J. Phys. C: Solid State Phys. **15**, L717 (1982).
- ³³ A. Crépieux and P. Bruno, cond-mat/0011426.
- ³⁴ J. Rammer, *Quantum transport theory* (Perseus Books, 1998) p. 322.
- ³⁵ In fact, a third series of diagrams gives a non-zero contribution at order $1/c^0$ to (29) but they are exactly compensated by opposite terms in $\bar{\sigma}^{II(0)}$, as discussed in Appendix B.